Baltic Astronomy, vol. 17, 223–234, 2008

IRC−10443: A MULTI-PERIODIC SRa VARIABLE AND THE NATURE OF LONG SECONDARY PERIODS IN AGB STARS

U. Munari[1], A. Siviero[1,3], P. Ochner[2], S. Dallaporta[2] and C. Simoncelli[2]

[1] *INAF Osservatorio Astronomico di Padova, via dell'Osservatorio 8, 36012 Asiago (VI), Italy*

[2] *ANS Collaboration, c/o Osservatorio Astronomico, via dell'Osservatorio 8, 36012 Asiago (VI), Italy*

[3] *Astrophysikalisches Institut Potsdam (AIP), An der Sternwarte 16, 14482 Potsdam, Germany*

Received 2008 August 30; revised September 3; accepted September 8

Abstract. We obtained BVI_C photometry of IRC−10443 on 85 different nights distributed over two years, and low resolution absolute spectrophotometry and high resolution Echelle spectroscopy. Our data show that IRC−10443, which was never studied before in detail, is an SRa variable, characterized by $\Delta B =$ 1.27, $\Delta V = 1.14$ and $\Delta I = 0.70$ mag amplitudes and mean values $< B > =$ 13.75, $< V > = 11.33$ and $< I_C > = 6.18$ mag. Two strong periodicities are simultaneously present: a principal one of 85.5 ($\pm$0.2) days, and a secondary one of 620 ($\pm$15) days, both sinusoidal in shape, and with semi-amplitudes $\Delta V = 0.41$ and 0.20 mag, respectively. We find that IRC−10443 is an M7 III star, with a mean heliocentric radial velocity −28 km/s and reddened by E_{B-V} = 0.87, a 1/3 of which of circumstellar origin. The same 0.5 kpc distance is derived from application of the appropriate period-luminosity relations to both the principal and the secondary periods. The long secondary period causes a sinusoidal variation of 0.13 mag semi-amplitude in the $V - I_C$ color, with the star being bluest at maximum and reddest at minimum, and with the associated changes in effective temperature and radius of 85 K and 6%, respectively. This behavior of colors argues in favor of a pulsation nature of the still mysterious long secondary periods in AGB stars.

Key words: stars: pulsations – stars: AGB – stars: variables: individual (IRC–10443)

1. INTRODUCTION

IRC−10443 (= RAFGL 2209 = NSV 11129 = BD–12 5123) is a bright (K=1.8 mag) infrared source discovered during the Two Micron Sky Survey (Neugebauer & Leighton 1969), that lies in the general direction of the Scutum Star Cloud. IRC−10443 was detected by the AFGL survey (Price & Murdock 1983) at 4.2 μm, and by IRAS satellite at 12 and 25 μm. Its 2MASS magnitudes and colors are K_s=1.92, $J - H$=1.35, $J - K$=1.80. Its spectral type is reported to be M6 by Neckel (1958) and Hansen & Blanco (1975), and M6.5 by Nassau et al. (1956). IRC−10443 is present in the NSV catalog of suspected variables because I-band observations, obtained at five different epochs (from 1963 August 21 to 1965 June 28) which are reported in the IRC catalog, seem to trace a variation from magnitude 6.4 to 6.9 (however, the uncertainty of the single measurement is similar to the dispersion of the five IRC measurements around their mean). Not much more is known about IRC−10443 and its nature. In this paper we report on our BVI photometric monitoring (85 nights distributed over two years) and optical spectroscopic observations (low and high resolution) of this object, and how they constrain its basic properties.

2. OBSERVATIONS

2.1. Photometry

$BVI_{\rm C}$ CCD photometry of IRC−10443 was independently obtained with two separate telescopes. The first one was the 0.3 m Meade RCX-400 f/8 Schmidt-Cassegrain telescope owned by Associazione Astrofili Valle di Cembra (Trento, Italy). The CCD was an SBIG ST-9, 512×512 array, 20 μm pixels and $1.72''$/pix, with a field of view of $13' \times 13'$. The B filter was from Omega and the $VI_{\rm C}$ filters from Custom Scientific. The second telescope was the 0.5 m f/8 Ritchey-Chretién telescope operated on top of Mt. Zugna by Museo Civico di Rovereto (Trento, Italy) and equipped with Optec $BVI_{\rm C}$ filters. The CCD was an Apogee Alta U42 2048×2048 array, 13.5 μm pixels and $0.70''$/pix, with a field of view of $24' \times 24'$.

The comparison star for the B and V passbands was TYC 5699-6341-1, for which we adopted B = 11.016 and V = 10.334 in the standard Johnson UBV system. They were obtained from Tycho $B_{\rm T}$,$V_{\rm T}$ data following Bessell (2000) transformations. The comparison star for the $I_{\rm C}$ passband was TYC 5699-6348-1 for which we adopted $I_{\rm C} = 6.39$ and $V - I_{\rm C} = 0.55$ from the *Hipparcos* catalog. We had no alternatives for the comparison stars. In fact, these two are the only stars within the CCD field of view of IRC−10443 that (*i*) have reference magnitudes available in literature, (*ii*) are bright enough to be well exposed on a single CCD image without risking to saturate IRC−10443, and (*iii*) are photometrically stable to better than 0.02 mag. The last point was verified by noting that on all frames in any passband we obtained that the relative magnitudes of the two comparison stars were stable at this level.

All photometric measurements were corrected for instrumental color equations derived nightly by the observations of Landolt (1992) standard fields. The good consistency of the data obtained independently with two different instruments reinforce our confidence in the accuracy of the results, in spite of the very red colors of IRC−10443, that are not reached by typical Landolt standard stars. Our photometry is presented in Table 1. It covers the period from 2006 July 16 to 2008 July 11, with observations collected on 85 different nights. The Poissonian component of the total error budget is less than 0.01 mag for all the data. The r.m.s. of the Landolt standard stars around the color equations they contributed to calibrate was on the average 0.019 mag for B, 0.022 for V and 0.031 for $I_{\rm C}$ passbands.

2.2. Spectroscopy

A low resolution, absolutely fluxed spectrum of IRC−10443 was obtained on 2008 June 24.97 UT with the B&C spectrograph of the INAF Astronomical Observatory of Padova attached to the 1.22 m telescope operated in Asiago by the Department of Astronomy of the University of Padova. The slit, aligned with the parallactic angle, projected onto $2''$ on the sky, and the total exposure time was

Table 1. Our CCD photometry of IRC−10443; *a* and *b* identify the telescopes described in Section 2.1.

HJD	B	V	I_C		HJD	B	V	I_C	
3935.366	13.78	11.39	6.05	*a*	4289.557	13.74	11.29	6.22	*b*
3955.386	13.73	11.31	6.19	*b*	4296.517	13.65	11.20		*b*
3966.387	13.75	11.42	6.24	*a*	4306.501		11.17	6.17	*b*
3970.385	13.85	11.41	6.27	*b*	4309.340	13.50	11.15	6.16	*b*
3975.370	13.90	11.49	6.30	*a*	4312.369	13.60	11.20	6.17	*b*
3988.311	13.96	11.58	6.33	*a*	4314.423	13.70	11.22	6.15	*b*
4007.263	14.03	11.57	6.32	*b*	4316.435	13.73	11.25	6.18	*b*
4014.273	13.89	11.46	6.24	*b*	4351.345	14.12	11.64	6.30	*b*
4015.245	13.81	11.42	6.31	*a*	4356.371	14.08	11.60	6.22	*b*
4017.256	13.89	11.40	6.19	*b*	4358.350	14.05	11.52	6.22	*b*
4019.287	13.73	11.36	6.26	*a*	4360.318	13.99	11.50	6.20	*b*
4019.296	13.70	11.37	6.18	*b*	4363.319	13.90	11.45	6.18	*b*
4024.299	13.59	11.20	6.16	*b*	4374.334	13.65	11.21	6.09	*b*
4035.233	13.28	10.95	6.00	*a*	4376.325	13.58	11.17	6.05	*b*
4035.295	13.32	10.94	5.94	*b*	4381.316	13.55	11.13	6.01	*b*
4042.238	13.23	10.88	5.95	*a*	4386.328	13.64	11.16	6.06	*b*
4042.286	13.25	10.82	5.83	*b*	4389.143	13.67	11.21	6.10	*b*
4043.247	13.24	10.84	5.85	*b*	4392.309	13.69	11.24	6.10	*b*
4062.203	13.70	11.22	6.08	*b*	4405.243	13.97	11.50	6.25	*b*
4067.185	13.75	11.32	6.08	*b*	4406.269	13.95	11.50	6.30	*b*
4071.190	13.84	11.42	6.09	*b*	4417.208	14.24	11.81	6.41	*b*
4080.191		11.50	6.16	*b*	4423.265	14.29	11.82		*b*
4081.193		11.51	6.22	*b*	4431.190	14.41	11.89	6.43	*b*
4151.717	13.71	11.43	6.18	*b*	4440.192	14.20	11.80	6.45	*b*
4158.690	14.04	11.62	6.45	*b*	4544.676	13.87	11.52	6.33	*b*
4168.660	14.05	11.63	6.39	*b*	4559.630	13.59	11.23	6.24	*b*
4174.657	14.00	11.59	6.36	*b*	4572.655	13.52	11.31	6.21	*b*
4181.629	13.96	11.50	6.28	*b*	4579.617	13.90	11.49	6.27	*b*
4193.576	13.70	11.24	6.13	*b*	4582.615	14.00	11.55	6.33	*b*
4196.595	13.61	11.17	6.13	*b*	4588.599	14.09	11.65	6.33	*b*
4196.644	13.59	11.16	6.08	*a*	4592.609	14.14	11.70	6.42	*b*
4201.585	13.40	10.96	6.01	*b*	4595.593	14.16	11.68	6.29	*b*
4201.652		11.00	6.01	*a*	4598.594	14.13	11.66	6.28	*b*
4204.614	13.29	10.89	5.95	*a*	4600.596	14.06	11.68	6.32	*b*
4207.638	13.23	10.80	5.92	*a*	4614.534	13.72	11.43	6.30	*b*
4210.633		10.80	5.96	*b*	4618.542	13.75	11.37	6.19	*b*
4211.635	13.14	10.75	5.88	*a*	4627.569	13.57	11.18	6.16	*b*
4218.634	13.21	10.83	5.92	*a*	4636.557	13.46	11.06	6.08	*b*
4229.609	13.65	11.14	6.09	*a*	4638.588	13.23	10.96	5.98	*b*
4231.588	13.74	11.23	6.08	*b*	4639.472	13.38	11.02	6.05	*b*
4239.586	13.92	11.43	6.25	*b*	4640.550	13.41	11.04	6.05	*b*
4239.590	14.03	11.42	6.22	*a*	4643.484	13.45	11.05	6.05	*b*
4260.579	14.18	11.82	6.45	*a*	4649.531	13.52	11.11	6.10	*b*
4275.512	14.16	11.70	6.35	*b*	4652.481	13.52	11.14		*b*
4287.503	13.80	11.35	6.23	*b*	4658.500	13.66	11.25	6.20	*b*
4288.549	13.82	11.34	6.26	*b*					

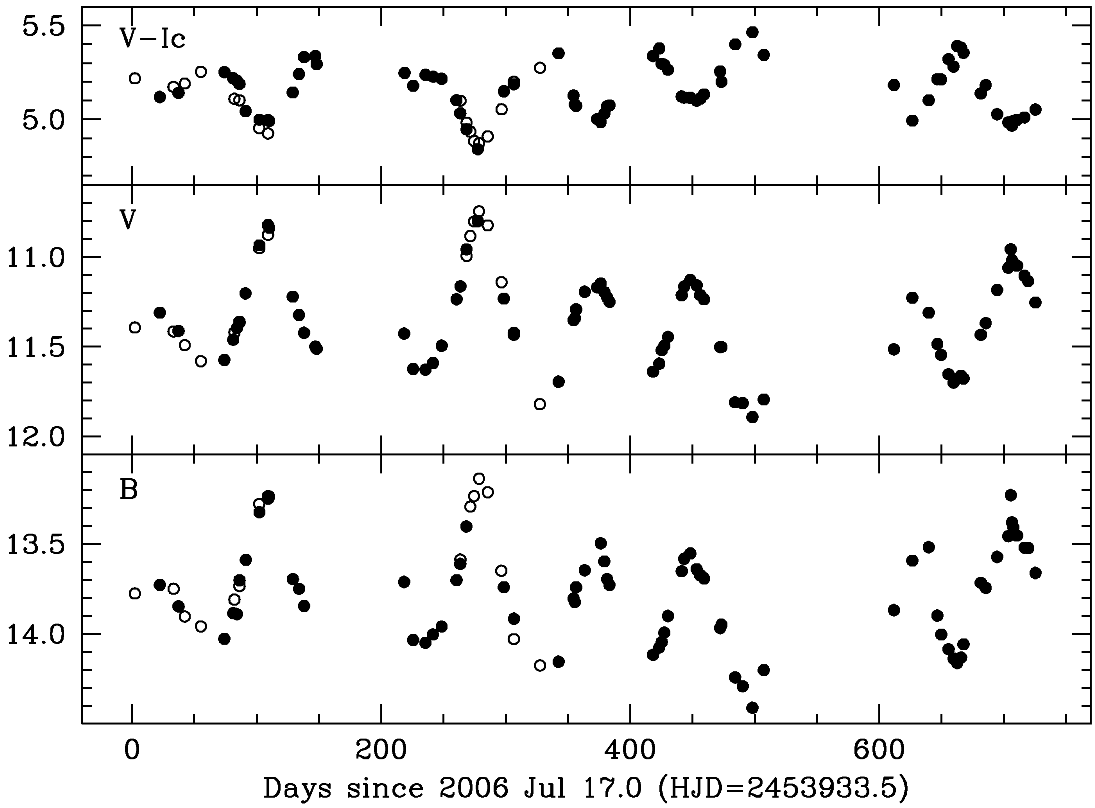

Fig. 1. Light- and color-curves of IRC 10443. Open circles: the 0.3 m telescope; dots: the 0.5 m telescope (see Section 2.1).

1860 sec. The detector was an ANDOR iDus 440A CCD camera, equipped with an EEV 42-10BU back illuminated chip, 2048×512 pixels of 13.5 μm size. A 300 ln/mm grating blazed at 5000 Å provided a dispersion of 2.26 Å/pix and a covered range extending from 3250 to 7890 Å.

High resolution spectra of IRC−10443 were obtained on 2008 June 10.04 and July 22.95 UT with the Echelle spectrograph mounted on the 1.82 m telescope operated in Asiago by INAF Astronomical Observatory of Padova. The detector was an EEV CCD47-10 CCD, 1024×1024 array, 13 μm pixel, covering the interval 3600−7300 Å in 31 orders. A slit width of 200 μm provided a resolving power R_P = 26 000.

3. RESULTS

3.1. Photometric variability

The light-curve presented in Figure 1 clearly shows that IRC−10443 is indeed variable. The recorded variability amounts to $\Delta B = 1.27$ (from 14.41 to 13.14), $\Delta V = 1.14$ (from 11.89 to 10.75) and $\Delta I_{\rm C} = 0.70$ (from 6.45 to 5.75), around the mean values $<B> = 13.75$, $<V> = 11.33$ and $<I_{\rm C}> = 6.18$ mag.

The variability is obviously periodic (see next section) and Figure 1 shows that the star gets hotter (bluest $V - I_{\rm C}$) at V maxima, and cooler (reddest $V - I_{\rm C}$) at V minima. This behavior of the color is a distinctive feature of stellar pulsation.

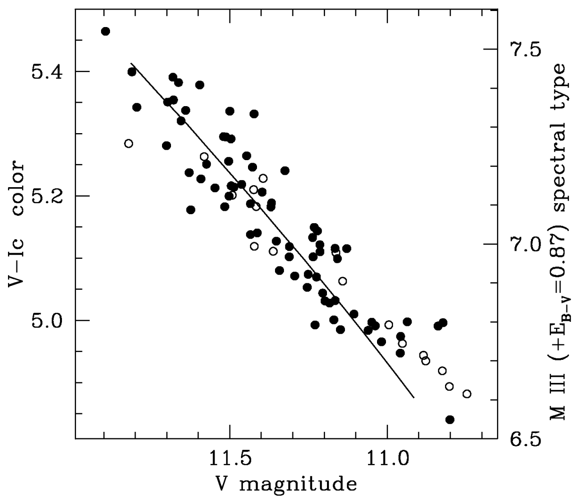

Fig. 2. Brightness vs. color diagram for the observations in Figure 1. The line is the path followed by a black-body, reddened by $E_{B-V} = 0.87$ and varying in radius and temperature at constant luminosity.

In fact, Figure 2 plots the $V - I_C$ color against the V magnitude, showing the clear correlation between them. If we take a black-body, redden it by $E_{B-V} = 0.87$, scale its flux so to match the average V band brightness of IRC−10443, and let it vary at constant luminosity, we obtain the line in Figure 2, which is a reasonably good fit to the observed points. This indicates that the variability displayed by IRC−10443 occurs at constant luminosity, in the form of expansion + cooling and contraction + warming, as expected in radial pulsations. The corresponding variation in spectral type is from M6.6 III to M7.5 III as indicated on the right ordinate axis of Figure 2. These corresponding spectral types have been obtained by convolving in the V and I_C bands the Fluks et al. (1994) spectra of M III giants reddened by $E_{B-V} = 0.87$ (the amount affecting IRC−10443, see Section 3.4).

IRC−10443 appears as a bona fide SRa variable. SRa variables are semi-regular late-type (M, C, S or Me, Ce, Se) giants displaying persistent periodicity and usually small ($\Delta V < 2.5$ mag) light amplitudes. Amplitudes and light-curve shapes generally vary and periods are in the range 35–1200 days. Many SRa stars differ from Miras only by showing smaller light amplitudes (Whitelock 1996).

3.2. Multi-periodicities

Two main periodicities at the same time are present in IRC−10443: a principal and larger amplitude variation modulated by a 85.5 day period, and a secondary and smaller one of 620 days. The following expression corresponds to the curve fitting the V-passband data in Figure 3 (where t is in HJD − 2450000):

$$V(t) = 11.38(\pm0.02) + 0.41(\pm0.02)\sin\frac{t - 4042.0(\pm0.3)}{85.5(\pm0.2)} +$$

$$+ 0.22(\pm0.02)\sin\frac{t - 4141(\pm10)}{620(\pm15)} \qquad (1)$$

The combination of these two plain sinusoids provides a reasonably close fitting to the observed light curve. Nevertheless, the residuals are larger than the observational errors, and an additional weaker component (either periodic or irregular) is probably present. Our present data are insufficient to characterize it – much longer photometric monitoring is required, which we plan to pursue.

3.3. Spectral classification and radial velocity

The low resolution spectrum of IRC−10443 was compared with the digital spectral atlas of Fluks et al. (1994), that includes all spectral types from M0 to

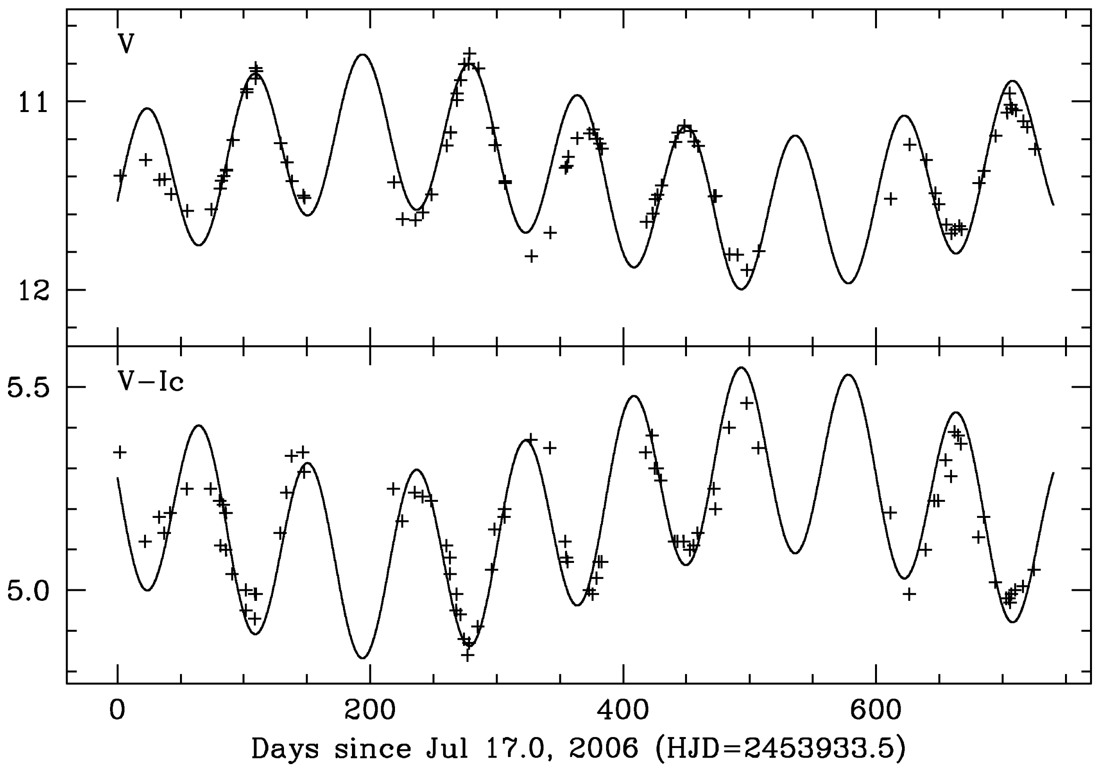

Fig. 3. Fitting of the V and $V - I_{\rm C}$ light curves of IRC−10443 with two sinusoids of 85.5 and 620 day periods (see Sections 3.2, 3.6 and Eq. 1).

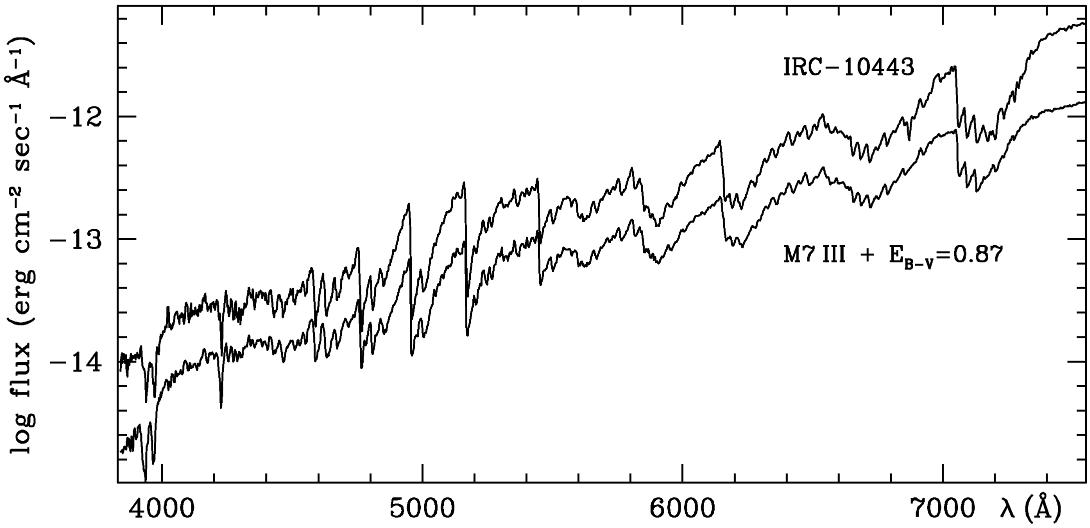

Fig. 4. Absolute spectrophotometry of IRC−10443 for 2008 June 24.97 UT (thick line) with superimposed the reference spectrum of a M7 III star from the atlas of Fluks et al. (1994) reddened by $E_{B-V} = 0.87$ (thin line).

M10 with spectra covering the whole optical range. They are of high flux accuracy and of a resolution similar to ours. The literature data suggest for IRC–10443 a spectral type of M6/M6.5, but our spectrum cannot be well fitted to the M6 III reference spectrum from the Fluks et al. (1994) library, while the match is perfect with the M7 III spectrum, as shown in Figure 4. In view of the pulsation activity of IRC−10443, the difference between our and other spectral classifications present in the literature can be accounted for by the changes in surface temperature during pulsations (see right hand-side ordinates of Figure 2).

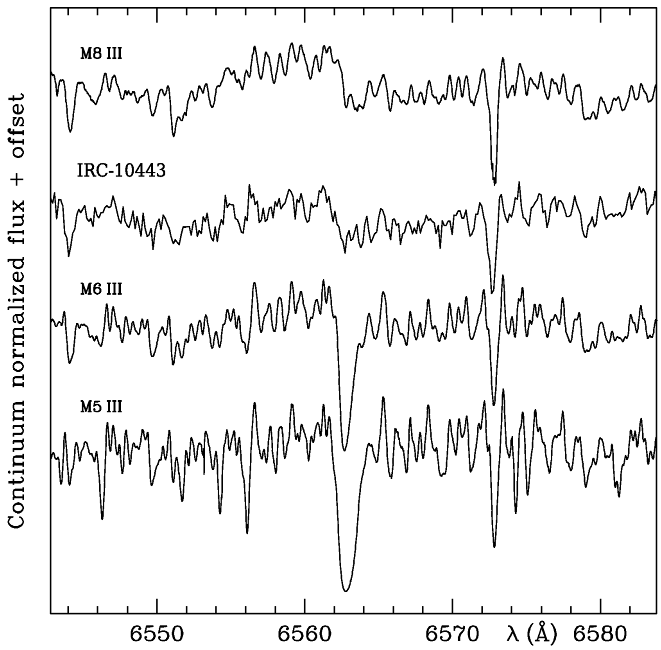

Fig. 5. A part of the high resolution Echelle spectrum of 2008 July 22.95, centered on Hα and Ca I 6572.8 Å. Spectra of cool giants from Bagnulo et al. (2003) are plotted for reference. All spectra are continuum normalized, shifted in ordinates for better visibility and shifted to zero radial velocity.

Figure 5 displays a portion of our high resolution Echelle spectrum centered on Hα of IRC−10443 obtained on July 22.95 For a comparison, the spectra of bracketing spectral types from the atlas of Bagnulo et al. (2003), degraded to the resolution of our Echelle spectrum via a Gaussian filter, are shown. The progression of spectral features in Figure 5 confirms the M7 III classification for IRC−10443.

Mira variables display emission lines, mainly the higher lines in the Balmer series, peaking in intensity at maximum brightness for both O- and C-rich varieties (e.g., Panchuk 1978; Yamashita et al. 1977; Mikulasek & Graf 2005), with large excursion in intensity along the pulsation cycle. When the first Echelle spectrum was exposed on June 10, IRC−10443 was on the rise and close to the maximum brightness (pulsation phase 0.86), while for the July 22 spectrum it was declining and close to the minimum brightness (pulsation phase 0.37). Both spectra do not show emission in the Hα line, in agreement with the fact that the presence of emission lines is far less frequent in SR than in Mira variables.

The radial velocity of IRC–10443 is −24.1(±0.8) and −31.4(±0.7) km/s on the June 10 and July 22 spectra, respectively. The difference is well accounted for by the pulsation activity. The two observations are separated in time by exactly half of the main 85.5 day pulsation period, and their mean value −28 km/s can be taken as representative of the systemic velocity of IRC−10443. At its Galactic coordinates ($\ell = 20°$, $b = -3°$) and distance (0.5 kpc, see below), the radial velocity expected from the Galactic disk rotation is +7 km/s (cf. also Brand & Blitz 1993). The 35 km/s difference with the observed radial velocity, suggests that IRC−10443 does not belong to the young disk population onto which it is seen projected, and instead it is probably related to an older population. This is confirmed by its high tangential velocity, 86 km/s, derived from the proper motion listed in the NOMAD catalog (Zacharias et al. 2004) and the distance estimated in Section 3.5 (below).

3.4. Reddening

The fit with the Flucks et al. (1994) M7 III reference spectrum presented in Figure 4 constrains the reddening affecting IRC−10443. The best match is obtained with $E_{B-V} = 0.87\pm0.02$ for a standard $R_V = 3.1$ reddening law.

The intrinsic B–V color of M giants almost does not depend on the spectral type and hence the effective temperature, as illustrated by Johnson (1966), Lee (1970) and Fitzgerald (1970). Their tabular compilations provide $<(B–V)_0> = +1.544$ as the mean intrinsic color of M5 to M8 luminosity III giants. The mean B–V color of our observations is $<(B–V)> = +2.418$, which corresponds to a reddening $E_{B-V} = 0.87\pm0.04$ affecting IRC–10443.

These two independent methods converge to the same amount of reddening affecting IRC–10443, $E_{B-V} = 0.87\pm0.03$, which is adopted in this paper. A fraction of this total reddening is probably of circumstellar origin, as supported by the detection by Kwok et al. (1997) of emission from circumstellar dust in IRAS low resolution spectra. IRC−10443 lies in the general direction of the Scutum Star Cloud (SSC, centered at $\ell = 27°$, $b = –3°$, Galactic coordinates). SSC is one of the regions of the Milky Way with the highest stellar density, caused by unusually low extinction over its area. Reichen et al. (1990) presented the results of a detailed investigation of the extinction over the SSC based on ground-based and balloon-born UV survey data. Toward the direction to IRC−10443 they found that the interstellar reddening linearly increases with distance until $E_{B-V} \approx 0.55$ is reached at 0.5 kpc. The further rise of the reddening with distance is very slow, reaching $E_{B-V} \approx 0.65$ at 4 kpc. Only for distances $d > 6$ kpc the reddening increases to $E_{B-V} \approx 1$ (Madsen & Reynolds 2005).

Following the results of Reichen et al. (1990), we therefore conclude that $\sim 1/3$ of the total $E_{B-V} = 0.87$ reddening affecting IRC−10443, is of probable circumstellar origin.

3.5. Distance

In a seminal paper, Wood et al. (1999) used MACHO observations of late-type giant variables in LMC to produce a period-luminosity diagram for them, where five separate period-luminosity sequences were identified. Comparing with the model prediction of Wood & Sebo (1996), three of these sequences were found to coincide with the fundamental and the first overtone pulsation modes, while the other two seemed to trace the variability induced by ellipsoidal distortion of RGB and AGB giants harbored in binary systems.

Since then, the availability of huge sets of data from large micro-lensing surveys (MACHO, OGLE, EROS, MOA) contributed to rapidly refine the picture, with now up to 14 different period-luminosity sequences identified (e.g., Kiss & Bedding 2003; Ita et al. 2004; Soszynski et al. 2005, 2007).

The most recent calibration of the various period-luminosity relations for late-type giant variables has been presented by Soszynski et al. (2007). Their relation for O-rich semi-regular variables of LMC takes the form $K_s = -4.35\,(\log P - 2.0) + 11.25$, where K_s passband corresponds to the 2MASS survey. Whitelock et al. (2008) have shown that any chemical abundance effect on the K-band period-luminosity relation of Miras must be small. Working with the revised *Hipparcos* parallaxes of van Leeuwen (2007), Whitelock et al. (2008) have derived that period-luminosity relation of O-rich Miras in our Galaxy has the same slope and it is 0.1 mag brighter than the corresponding one for the LMC. We assume that a similar 0.1 mag shift would make the Soszynski et al. (2007) relations applicable to the O-rich SRa variables of our Galaxy. Adopting this 0.1 mag shift, an LMC distance modulus of $(m–M)_0 = 18.39$ (van Leeuwen et al. 2007), an LMC reddening of $E_{B-V} = 0.06$ (Mateo 1998), the extinction relation $A_{K_s} = 0.442\,E_{B-V}$ for a spectral distribution of M-type star and the standard $R_V = 3.1$ extinction law (Fiorucci & Munari 2003), the distance to IRC−10443 corresponding to the 85.5 day period is 0.5 kpc. The Soszynski et al. (2007) relation for the long secondary periods of O-rich red giants in LMC takes the form $K_s = -4.41(\log P - 2.0) + 15.05$, and when applied (with the same 0.1 mag shift as above) to the 620 day secondary period of IRC−10443, it provides the same distance, 0.5 kpc, as obtained for the 85.5 day main period. In this paper we accept this value of distance to IRC–10443.

3.6. On the nature of the long secondary period

In spite of large investigation efforts, both observational and theoretical, "*the cause of the long secondary periods seen in cool giants remains a mystery at the present time*" as was recently remarked by Wood (2007).

It is known that some semi-regular variables show the presence of long secondary periods (LSPs) in their light curves, typically ten times longer than the primary pulsation period. For IRC−10443 this ratio is 7.25. Lists of local giants displaying LSPs have been published, among others, by Houk (1963), Mattei et al. (1997), Kiss et al. (1999). Wood et al. (1999) found that in LMC $\sim$25% of all variable AGB stars show LSPs. A similar fraction, $\sim$30%, was found for the local semi-regular variables by Percy et al. (2004).

The semi-regular variables appear to pulsate in the first overtone (Lebzelter & Wood 2006), and thus it could be tempting to relate the LSPs with pulsation in the fundamental mode. However, as found in theoretical models by Fox & Wood (1982) and verified by observations (e.g., Kiss et al. 1999; Mattei et al. 1997), the ratio of fundamental to first overtone periods is close to two, ruling out that LSPs are due to pulsations in the fundamental mode. The established observational facts are in favor that LSPs are accompanied by radial velocity variations (of a lower amplitude than observed for the primary period; Hinkle et al. 2002; Wood et al. 2004) and by variation in intensity of the Hα absorption (that could trace a variable filling by an emission component of chromospheric origin; Wood et al. 2004). In addition, cool variable giants showing LSPs rotate at similar velocity and show similar dust-free IRAS colors as cool variable giants without LSPs (Olivier & Wood 2003). In the RGB objects showing LSPs, the period of associated radial velocity variations is twice the period of photometric LSP variability (as expected in the case LSPs arise from ellipsoidally distorted giants in binary systems; Adams et al. 2006), while in the AGB objects the period is the same (as expected in the case of pulsations; Wood et al. 2004). Various explanations of the LSP phenomenon have been proposed, but all have encountered some problems, as discussed by Wood (2007 and references therein).

A striking feature displayed by IRC−10443 is illustrated in the bottom panel of Figure 3, where the color variation is fitted with two sinusoids of the same periods of those fitting the V light-curve (cf Eq. 1 and the top-panel of Figure 3). Their semi-amplitudes are 0.23 mag for the sinusoid associated to the principal 85.5 day period, and 0.13 mag for the LSP, with a mean $V - I_{\rm C} = 5.19$. From Figure 3 it is evident that IRC−10443 is the bluest when it is at the maximum brightness along the LSP cycle, and reddest when it is at the minimum brightness. This is the same pattern observed for the principal 85.5 day period and strongly argues in favor of a pulsation interpretation of the LSP phenomenon, at least in IRC−10443. The simultaneous presence of two pulsations also accounts for the dispersion of points in Figure 2 along the back-body curve. The dispersion would have been significantly reduced if only one pulsation would be present, as is confirmed by removing from observations one or the other of the sinusoidal variation of the color and re-plotting Figure 2.

The variation in the $V - I_{\rm C}$ color can be transformed into variation in effective temperature of the underlying stellar photosphere using the reference continuum energy distribution given by Fluks et al. (1994) along the spectral sequence of M giants. The total amplitude of 0.46 mag observed in $V - I_{\rm C}$ for the principal period, corresponds to a change in 0.73 of spectral subclass around the M7 III mean, and therefore to a variation from 3030 to 3175 K in effective temperature. The 0.26 mag total color amplitude of the LSP would correspond to a change of 0.41 of spectral subclass around the M7 III mean, which means the variation of $T_{\rm eff}$ from 3060 to 3145 K. If both pulsations are supposed to occur at constant luminosity, the corresponding total excursion in radius is $\sim 10\%$ for the principal 85.5 day period, and $\sim 6\%$ for the LSP.

These excursions in radius are less than that inferred by Wood et al. (2004) from radial velocity observations at the optical wavelengths of a sample of three hotter AGB stars characterized by longer LSP than IRC−10443. We estimated the change in *effective* temperature and radius of the underlying photosphere. If instead we had referred to a black-body fitting of the observed optical spectrum of the star (re-shaped by extremely strong TiO molecular absorptions), the variation in *color* temperature and radius of IRC−10443 would have been almost twice larger, 150 K and 10 %, respectively.

It is worth noticing that recent theoretical improvements in the treatment of pulsation, like inclusion of time-dependent turbulent convection (Olivier & Wood 2006), are opening new modeling possibilities for pulsation modes in cool giants. Important applications to the long-lasting problem of what is driving the LSPs could be obtained in the near future (cf. Wood 2006). To better characterize the object and increase its interest as a test target for current theories, we plan to continue a tight observational monitoring of IRC−10443 over the next years, long enough to cover at least the whole next LSP period.

ACKNOWLEDGMENTS. We would like to thank P. A. Whitelock for useful comments on the original version of the paper, the anonymous referee for helpful suggestions, and S. Ciroi, F. Di Mille, S. Tomasoni, F. Moschini and M. Nave for assistance during the observations.

REFERENCES

Adams E., Wood P. R., Cioni M. R. 2006, MSAIt, 77, 537
Bagnulo S., Jehin E., Ledoux C. et al. 2003, The Messenger, 114, 1
Bessell M. S. 2000, PASP, 112, 961
Brand J., Blitz L. 1993, A&A, 275, 67
Fiorucci M., Munari U. 2003, A&A, 401, 781
Fitzgerald M. P. 1970, A&A, 4, 234
Fluks M. A., Plez B., The P. S. et al. 1994, A&AS, 105, 311
Fox M. W., Wood P. R. 1982, ApJ, 259, 198
Ita Y., Tanabe T., Matsunaga N. et al. 2004, MNRAS, 353, 705
Johnson H. L. 1966, ARA&A, 4, 193
Hansen O. L., Blanco V. M. 1975, AJ, 80, 1011
Hinkle K. H., Lebzelter T., Joyce R. R., Fekel F. C. 2002, AJ, 123, 1002
Houk N. 1963, AJ, 68, 253
Kiss L. L., Szatmáry K., Cadmus R. R., Mattei J. A. 1999, A&A, 346, 542
Kiss L. L., Bedding T. R. 2003, MNRAS, 343, L79
Kwok S., Volk K., Bidelman W. P. 1997, ApJS, 112, 557
Landolt A. U. 1992, AJ, 104, 340
Lebzelter T., Wood P. R. 2006, MSAIt, 77, 55
Lee T. A. 1970, ApJ, 162, 217
Madsen G. J., Reynolds R. J. 2005, ApJ, 630, 925
Mateo M. L. 1998, ARA&A, 36, 435
Mattei J. A., Foster G., Hurwitz L. A. et al. 1997, in *Hipparcos – Venice '97*, ESA SP-402, 269
Mikulášek Z., Gráf T. 2005, Contrib. Obs. Skalnaté Pleso, 35, 83
Nassau J. J., Blanco V. M., Cameron D. M. 1956, ApJ, 124, 522
Neckel H. 1958, ApJ, 128, 510
Neugebauer G., Leighton R. B. 1969, *Two-Micron Sky Survey. A Preliminary Catalogue*, NASA SP-3047, Washington
Olivier E. A, Wood P. R. 2003, ApJ, 584, 1035
Olivier E. A, Wood P. R. 2006, MSAIt, 77, 515
Panchuk V. E. 1978, SvAL, 4, 201
Percy J. R., Bakos A. G., Besla G. et al. 2004, in *Variable Stars in the Local Group*, IAU Colloq. 193, eds. D. W. Kurtz & K. R. Pollard, ASPC, 310, 348
Price S. D., Murdock T. L. 1983, *The Revised AFGL I.R. Sky Survey, Catalog and Supplement*, Air Force Geophysics Lab., AFGL-IR-83-0161
Reichen M., Lanz T., Golay M., Huguenin D. 1990, Ap&SS, 163, 275
Soszynski I., Udalski A., Kubiak M. et al. 2005, AcA, 55, 331
Soszynski I., Dziembowski W. A., Udalski A. et al. 2007, AcA, 57, 201
van Leeuwen F. 2007, *Hipparcos: The New Reduction of the Raw Data*, Springer-Verlag
van Leeuwen F., Feast M. W., Whitelock P. A., Laney C. D. 2007, MNRAS, 379, 723
Yamashita Y., Nariai K., Norimoto Y. 1977, *An Atlas of Representative Stellar Spectra*, Univ. of Tokyo Press
Whitelock P. A. 1996, in *Light Curves of Variable Stars*, eds. C. Sterken & C. Jaschek, Cambridge Univ. Press

Whitelock P. A., Feast M. W., van Leeuwen F. 2008, MNRAS, 386, 313
Wood P. R., Sebo K. M. 1996, MNRAS, 282, 958
Wood P. R., Alcock C., Allsman R. A. et al. 1999, in *Asymptotic Giant Branch Stars*, IAU Symp. 191, eds. T. Le Bertre, A. Lebre & C. Waelkens, p. 151
Wood P. R., Olivier E. A., Kawaler S. D. 2004, ApJ, 604, 800
Wood P. R. 2006, MSAIt, 77, 76
Wood P. R. 2007, in *The 7th Pacific Rim Conference on Stellar Astrophysics*, eds. Y. W. Kang et al., ASPC, 362, 234
Zacharias N., Monet D. G., Levine S. E. et al. 2004, AAS, 205, 4815